CHAPTER IV
RESULTS AND DISCUSSION

4.1 Reaction Activity Performance under Dielectric Barrier Discharge

4.1.1 Effect of Molar Ratio of O_2/C_2H_4

The effect of feed molar ratio was initially studied in order to obtain the most suitable feed gas composition for ethylene epoxidation reaction under the low-temperature dielectric barrier discharge system. To better understand the influence of the feed gas composition, the effect of O_2/C_2H_4 molar ratio was investigated in the range of 1/1 to 4/1. The applied voltage of 17 kV and input frequency of 550 Hz were applied during the reaction.

4.1.1.1 Effect of Molar Ratio of O_2/C_2H_4 on Ethylene and Oxygen Conversions, Ethylene Oxide Yield, and Product Selectivities

The effect of O_2/C_2H_4 molar ratio on the C_2H_4 and O_2 conversions and the C_2H_4O yield is shown in Figure 4.1, and the selectivities for C_2H_4O, CO, CO_2, H_2, CH_4, C_2H_2, C_2H_6, and C_3H_8 are shown in Figure 4.2. The increase in the O_2/C_2H_4 molar ratio slightly affected the reactant conversions, but it mainly affected the CO_2 selectivity, especially at the ratio of O_2/C_2H_4 above 2/1. This can be explained in that the higher O_2/C_2H_4 ratio led to more O_2 content available to react with various hydrocarbon molecules, as well as C_2H_4O and CO, to convert to CO_2. However, the conversion of O_2 reached a maximum in the molar ratio range between 2/1 and 3/1, which is about the theoretical ratio for C_2H_4 complete combustion, as shown in Equation 4.1. At the molar ratio higher than 3/1 or excess O_2 condition, the conversion of O_2 tended to decrease since O_2 was probably consumed at the same level while initial amount of O_2 was higher.

$$C_2H_4 + 3O_2 \rightarrow 2CO_2 + 2H_2O \qquad (4.1)$$

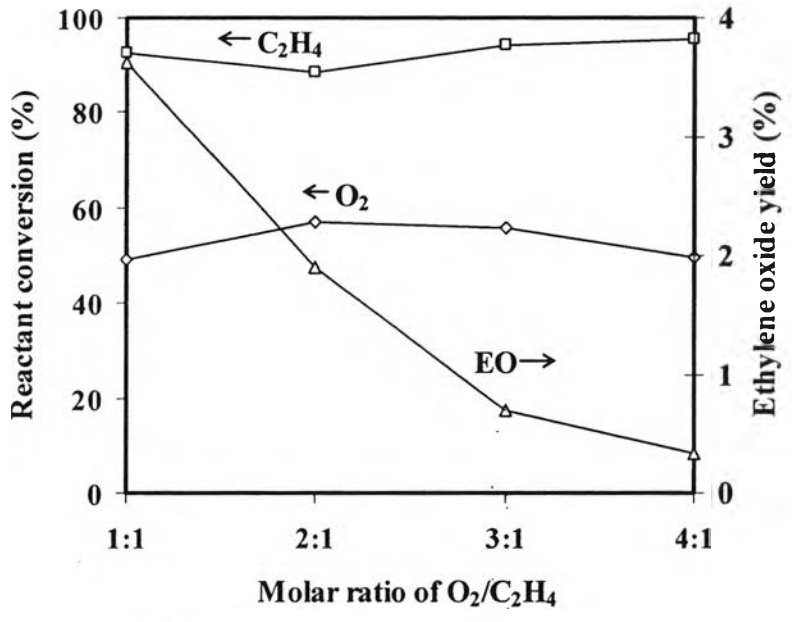

Figure 4.1 Conversions of ethylene and oxygen and yield of ethylene oxide as a function of O_2/C_2H_4 molar ratio (feed flow rate = 50 cm^3/min; electrode gap distance = 10 mm; applied voltage = 17 kV; and input frequency = 550 Hz).

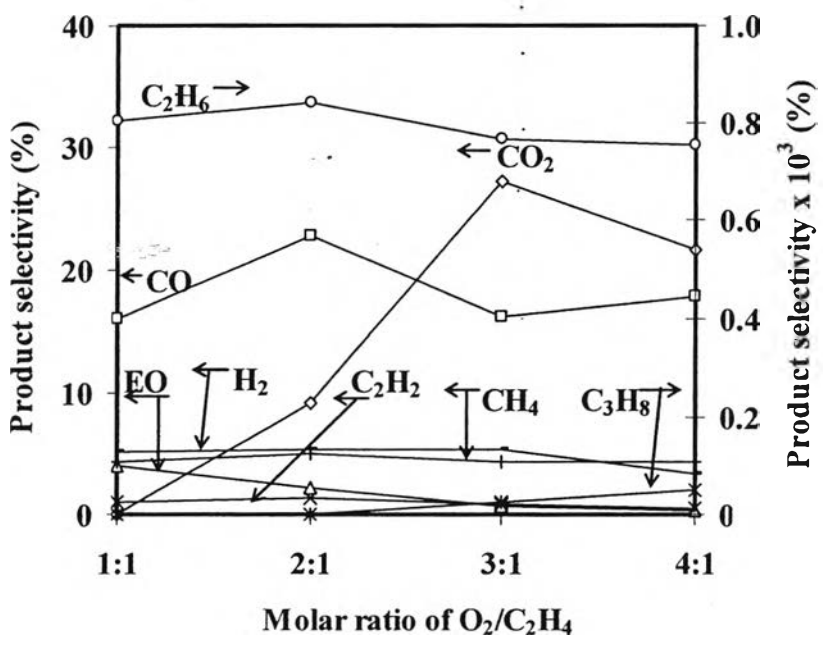

Figure 4.2 Product selectivities as a function of O_2/C_2H_4 molar ratio (feed flow rate = 50 cm^3/min; electrode gap distance = 10 mm; applied voltage = 17 kV; and input frequency = 550 Hz).

In this DBD system, the yield of C_2H_4O and the selectivities for C_2H_4O, H_2, C_2H_2, and C_2H_6 tended to decrease, but in contrast, the selectivity for CO_2 increased with increasing the O_2/C_2H_4 molar ratio, as aforementioned. Interestingly, the selectivity for CH_4 remained almost constant. At molar ratio of O_2/C_2H_4 equal to 2/1, O_2 was contributed to form the highest amount of CO. At the molar ratio higher than 2/1, excess O_2 was employed for complete oxidation of CO and hydrocarbons (C_2H_2 and C_2H_6), resulting in higher amount of CO_2, and a maximum CO_2 selectivity was observed at the ratio of 3/1, which is the theoretical ratio for C_2H_4 complete combustion The decrease in the selectivities for these hydrocarbons and H_2 with the increases in the selectivity for CO_2 clearly reveals that the oxidative dehydrogenation and coupling reactions unfavorably occurred under O_2-rich conditions, as expected. It must be also noted that there was no detectable CO_2 when using the O_2/C_2H_4 molar ratio of 1/1, which was chosen for all further experiments under all conditions. Furthermore, at a higher O_2/C_2H_4 molar ratio, the selectivity for C_2H_4O dropped to zero level since this higher molar ratio of O_2/C_2H_4 led to the complete combustion to occur more favorably than partial oxidation, indicating that the epoxidation reaction to produce C_2H_4O was more likely to occur under O_2-lean conditions.

4.1.1.2 Comparison of Specific Power Consumption for Different Molar Ratios of O_2/C_2H_4

Figure 4.3 shows the power consumptions used to convert ethylene molecule and to produce ethylene oxide molecule at different O_2/C_2H_4 molar ratios. The power consumption per molecule of converted ethylene reached a maximum when the O_2/C_2H_4 molar ratio increased up to 2/1 and slightly decreased with further increasing the molar ratio. However, there was a significant increase in the power consumption per molecule of produced ethylene oxide with increasing O_2/C_2H_4 molar ratio, especially at the molar ratio higher than 3/1. It can also be noticed that since the power consumption per molecule of ethylene oxide produced was approximately two orders of magnitude higher than that per molecule of ethylene converted, the former must be taken into much more consideration. An O_2/C_2H_4 molar ratio of 1/1 was therefore selected for further experiments because it

provided the highest selectivity and yield for ethylene oxide and the lowest power consumption per molecule of ethylene oxide produced.

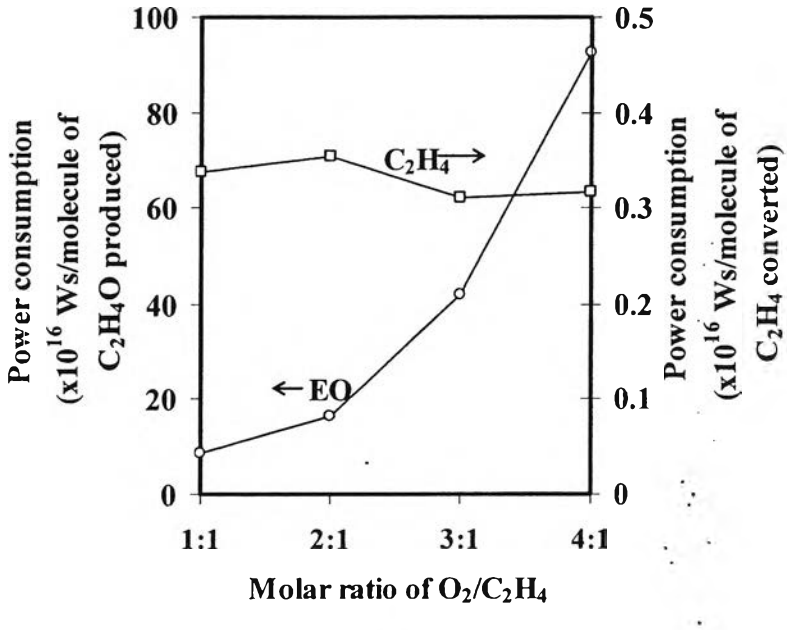

Figure 4.3 Comparison of specific power consumptions for different O_2/C_2H_4 molar ratios (feed flow rate = 50 cm^3/min; electrode gap distance = 10 mm; applied voltage = 17 kV; and input frequency = 550 Hz):

4.1.2 Effect of Feed Flow Rate

The feed flow rate plays a significant role on the residence time of gas molecules within the plasma zone, affecting the performance of the plasma system. The experiments were performed by varying feed flow rate from 50 to 125 cm^3/min. At a feed flow rate lower than 50 cm^3/min, the O_2 flow rate cannot be adjusted due to the limitation of a mass flow controller. An O_2/C_2H_4 molar ratio of 1/1, an applied voltage of 17 kV, and an input frequency of 550 Hz were applied during the reaction.

4.1.2.1 Effect of Feed Flow Rate on Ethylene and Oxygen Conversions, Ethylene Oxide Yield, and Product Selectivities

Figure 4.4 illustrates the influences of the feed flow rate on the C_2H_4 and O_2 conversions. The conversion of O_2 gradually decreased with increasing the feed flow rate from 50 to 125 cm^3/min while the conversion of C_2H_4

more sharply decreased. An increase in the feed flow rate generally reduces the gas residence time in the reaction system, resulting in having a shorter contact time of ethylene and oxygen molecules to collide with electrons. As a result, a reduction in the feed flow rate enhanced the conversions of both C_2H_4 and O_2, which led to an increase in the yield of C_2H_4O, as also shown in Figure 4.4.

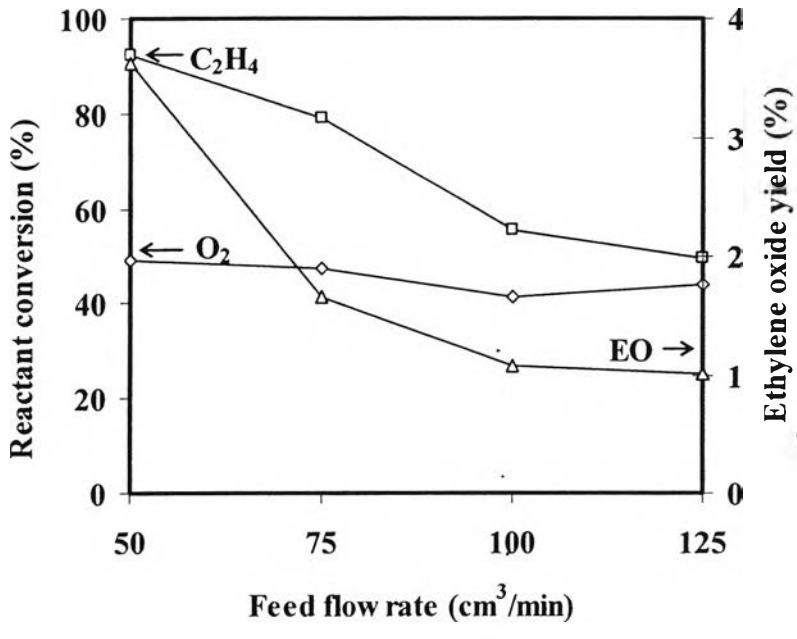

Figure 4.4 Conversions of ethylene and oxygen and yield of ethylene oxide as a function of feed flow rate (molar ratio of O_2/C_2H_4 = 1/1; electrode gap distance = 10 mm, applied voltage = 17 kV, and input frequency = 550 Hz).

The feed flow rate dependence of product selectivities is depicted in Figure 4.5. It is apparent that increasing feed flow rate resulted in a decrease in the selectivities for C_2H_4O and CO. This is because a higher feed flow rate reduces the opportunity of collision between electrons and reactant/intermediate molecules. But for other products, especially C_2H_2 and C_3H_8, their selectivities tended to increase because a shorter residence time at higher feed flow rate probably enabled the oxidative dehydrogenation and coupling reaction more favorable to occur than partial oxidation.

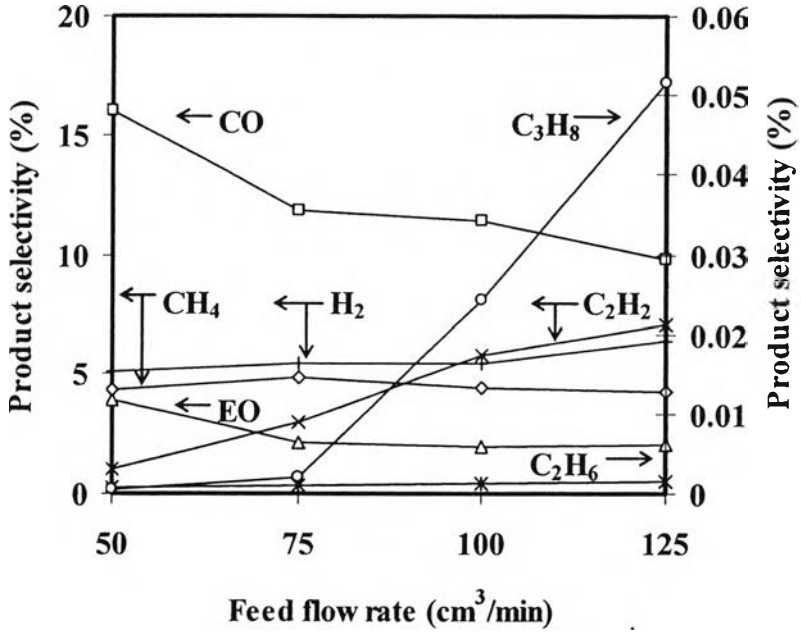

Figure 4.5 Product selectivities as a function of feed flow rate (molar ratio of O_2/C_2H_4 = 1:1; electrode gap distance = 10 mm; applied voltage = 17 kV; and input frequency = 550 Hz).

4.1.2.2 Comparison of Specific Power Consumption for Different Feed Flow Rates

Figure 4.6 shows the effect of feed flow rate on the power consumptions. The power consumption per molecule of converted ethylene slightly decreased, but the power consumption per molecule of produced ethylene oxide tended to greatly increase when increasing feed flow rate. The lower feed flow rate gave comparatively low power consumption per molecule of produced ethylene oxide, as well as much higher reactant conversions and desired product selectivity. Therefore, the feed flow rate of 50 cm^3/min was selected as an optimum value and used for further experiments.

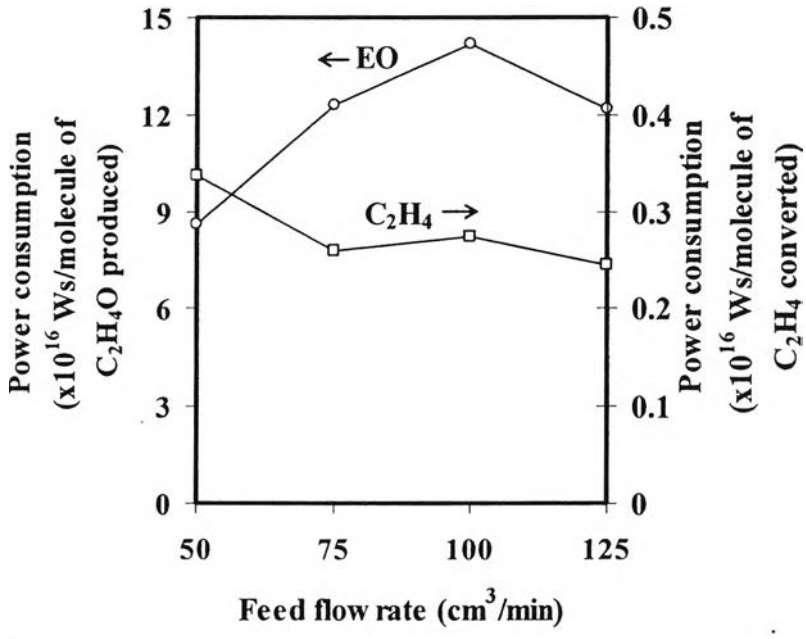

Figure 4.6 Comparison of specific power consumptions for different feed flow rates (molar ratio of O_2/C_2H_4 = 1/1; electrode gap distance = 10 mm; applied voltage = 17 kV; and input frequency = 550 Hz).

4.1.3 Effect of Input Frequency

Input frequency is one of the most important parameter in plasma reactor operation, significantly affecting the field strength in the plasma zone. The studied DBD system was operated in the frequency range of 500-800 Hz. At a frequency lower than 500 Hz, the plasma distribution was not fairly uniform over the whole electrode surface, and it tended to appear as a single strong stream of plasma discharge, whereas the plasma could not exist at a frequency higher than 800 Hz.

4.1.3.1 Effect of Input Frequency on Ethylene and Oxygen Conversions, Ethylene Oxide Yield, and Product Selectivities

The effect of input frequency on the C_2H_4 and O_2 conversions and yield of C_2H_4O is illustrated in Figure 4.7. When increasing input frequency in the range of 500-650 Hz, the O_2 and C_2H_4 conversions and C_2H_4O yield decreased dramatically. And, they turned to slightly decrease with further increasing input frequency up to 800 Hz. The explanation is that a higher frequency results in a lower

current that corresponds to the reduction of the number of electrons generated (weaker field strength), as shown in Figure 4.8. It therefore caused the decrease in amount of active species for further reactions, resulting in the decrease in the C_2H_4 and O_2 conversions and subsequently leading to the lower yield of C_2H_4O.

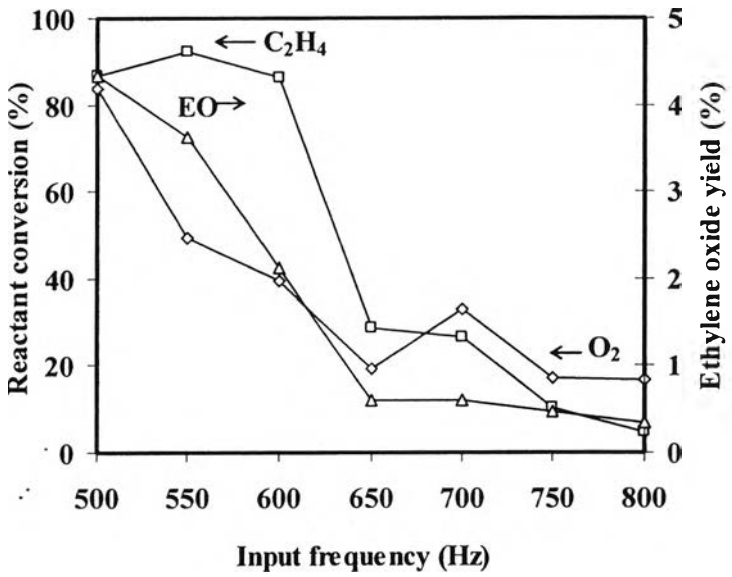

Figure 4.7 Conversions of ethylene and oxygen and yield of ethylene oxide as a function of input frequency (molar ratio of O_2/C_2H_4 = 1/1; feed flow rate = 50 cm^3/min; electrode gap distance = 10 mm; and applied voltage = 17 kV).

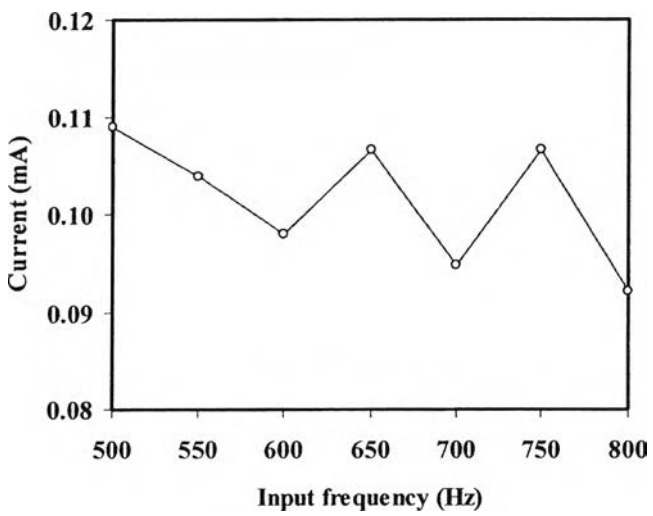

Figure 4.8 Effect of input frequency on generated current (molar ratio of O_2/C_2H_4 = 1/1; feed flow rate = 50 cm^3/min; electrode gap distance = 10 mm; and applied voltage = 17 kV).

The effect of input frequency on the product selectivities is shown in Figure 4.9. The selectivities for C_2H_4O and CO tended to slightly decrease with increasing input frequency until 650 Hz. At a higher frequency than 650 Hz, partial oxidation, oxidative dehydrogenation, and coupling reactions to form various products increasingly occurred. Particularly, the selectivity for CO significantly increased. The selectivity for C_2H_4O also gradually increased to reach a maximum of 7.3% at 800 Hz for high frequency range between 650-800 Hz, as compared with 5.0% at 500 Hz for low frequency range between 500-650 Hz. However, the input frequency of 500 Hz was considered as a potentially optimum value, exhibiting the highest C_2H_4O yield with a reasonably high C_2H_4O selectivity and a relatively low CO selectivity.

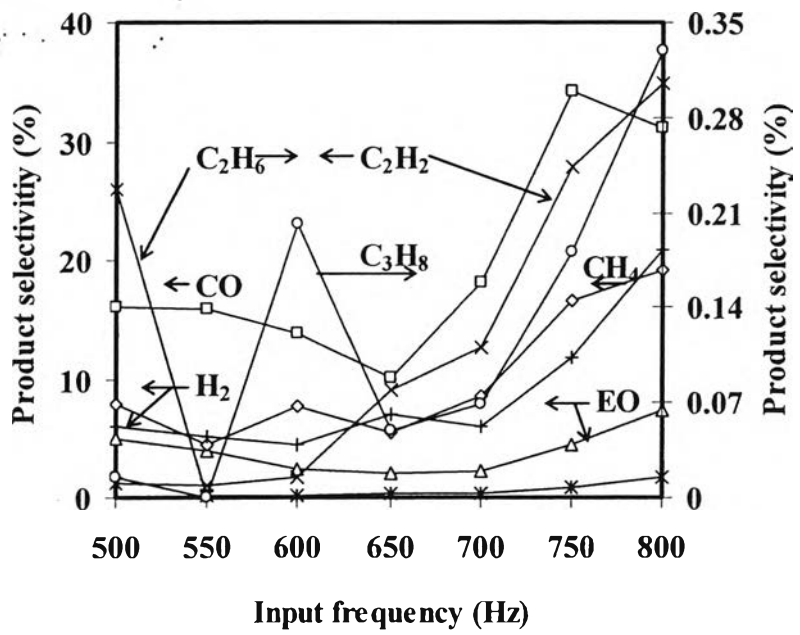

Figure 4.9 Product selectivities as a function of input frequency (molar ratio of O_2/C_2H_4 = 1/1; feed flow rate = 50 cm^3/min; electrode gap distance = 10 mm; and applied voltage = 17 kV).

4.1.3.2 Comparison of Specific Power Consumption for Different Input Frequencies

The effect of input frequency on the power consumptions to break down each C_2H_4 molecule and to create each C_2H_4O molecule is shown in Figure 4.10. The results show that both the power consumptions per C_2H_4 molecule converted and per C_2H_4O molecule produced tended to increase with increasing input frequency, especially at input frequency higher than 600 Hz. Hence, the optimum input frequency was considered to be at 500 Hz. Again, based upon relatively high ethylene oxide yield and the lowest power consumption per molecule of ethylene oxide produced, the optimum input frequency of 500 Hz was selected for further experiments.

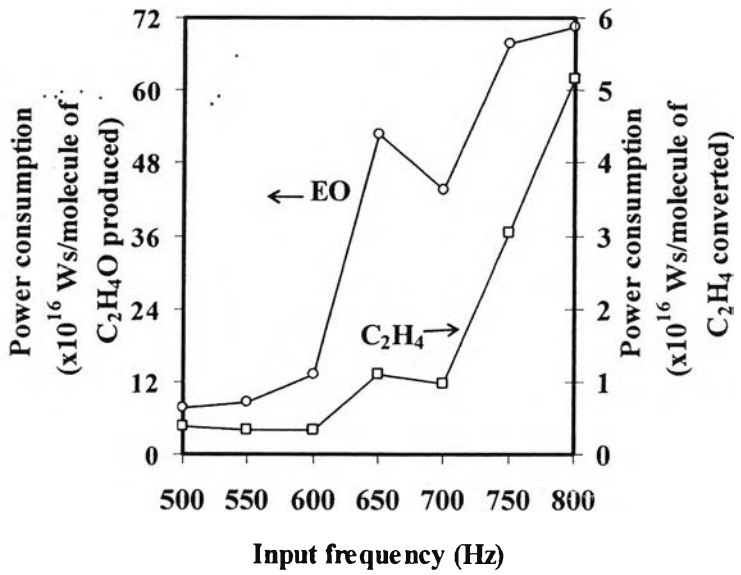

Figure 4.10 Comparison of specific power consumptions for different input frequencies (molar ratio of O_2/C_2H_4 = 1/1; feed flow rate = 50 cm^3/min; electrode gap distance = 10 mm; and applied voltage = 17 kV).

4.1.4 Effect of Applied Voltage

Under the studied conditions, the break-down voltage or the lowest voltage (onset voltage) to generate plasma was found to be about 13 kV, and the DBD system could not be operated at the applied voltage higher than 21 kV since the

generated plasma was found to have the non-uniform distribution characteristic. Therefore, the reaction experiments were conducted in the voltage range of 13-21 kV in order to determine the effect of the applied voltage.

4.1.4.1 Effect of Applied Voltage on Ethylene and Oxygen Conversions, Ethylene Oxide Yield, and Product Selectivities

The effect of applied voltage on the C_2H_4 and O_2 conversions and C_2H_4O yield is illustrated in Figure 4.11. The oxygen conversion and C_2H_4O yield tended to considerably increase with increasing applied voltage in the range of 13-19 kV, whereas the ethylene conversion only gradually increased. With further increasing applied voltage higher than 19 kV, the reactant conversions and the C_2H_4O yield did not significantly change. The explanation of more rapid increment in the O_2 conversion is that a higher voltage results in a higher current (stronger field strength), as shown in Figure 4.12, leading to more available electrons to increase an opportunity for collision with oxygen. In contrast, it is unexpected that the C_2H_4 conversion only gradually increased with increasing applied voltage. This can be explained in that the bond dissociation energy of C_2H_4 (16.7 eV) is much higher than that of O_2 (12.2 eV), particularly causing O_2 molecule easier to be converted than C_2H_4 under relatively stronger field strength at a higher voltage.

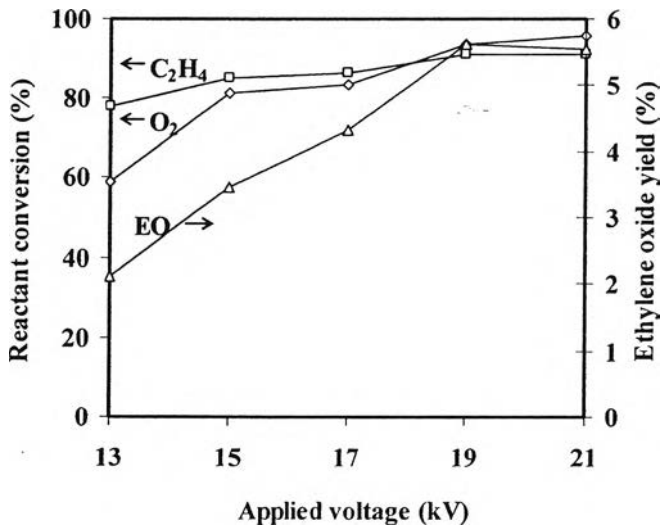

Figure 4.11 Conversions of ethylene and oxygen and yield of ethylene oxide as a function of applied voltage (molar ratio of O_2/C_2H_4 = 1/1; feed flow rate = 50 cm^3/min; electrode gap distance = 10 mm; and input frequency = 500 Hz).

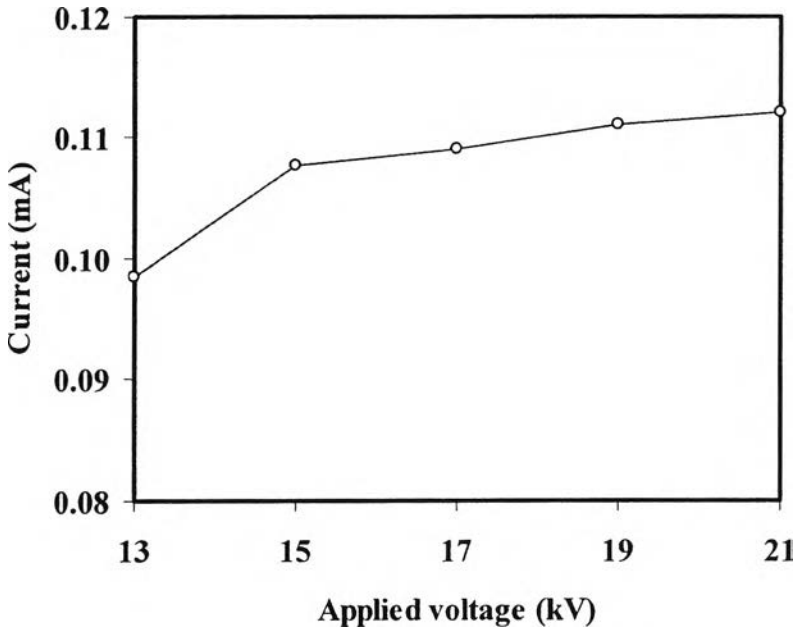

Figure 4.12 Effect of applied voltage on generated current (molar ratio of O_2/C_2H_4 = 1/1; feed flow rate = 50 cm^3/min; electrode gap distance = 10 mm; and input frequency = 500 Hz).

The effect of applied voltage on the selectivities for C_2H_4O, CO, H_2, CH_4, C_2H_2, C_2H_6, and C_3H_8 is shown in Figure 4.13. The selectivities for C_2H_4O, CO, H_2, and other hydrocarbon products, except C_2H_2 selectivity, increased with increasing applied voltage. When the applied voltage increased, corresponding to increasing O active species as mentioned above, active hydrocarbon species were further oxidized to form more CO and C_2H_4O in the plasma environment, but CO was not further oxidized to CO_2 due to no CO_2 detectable. These results suggest that higher amount of O active species at higher applied voltage is more favorable for C_2H_4O production than complete combustion. Only the selectivity for C_2H_2 was observed to decrease when increasing applied voltage. This might be because the formed C_2H_2 might further react with largely available O active species to form other products more easily. Interestingly, the further increase in applied voltage higher than 19 kV did not help enhance the C_2H_4O production. The applied voltage of 19 kV might be efficiently sufficient for the desired product formation, and the excess power input due to further increasing input voltage is not required.

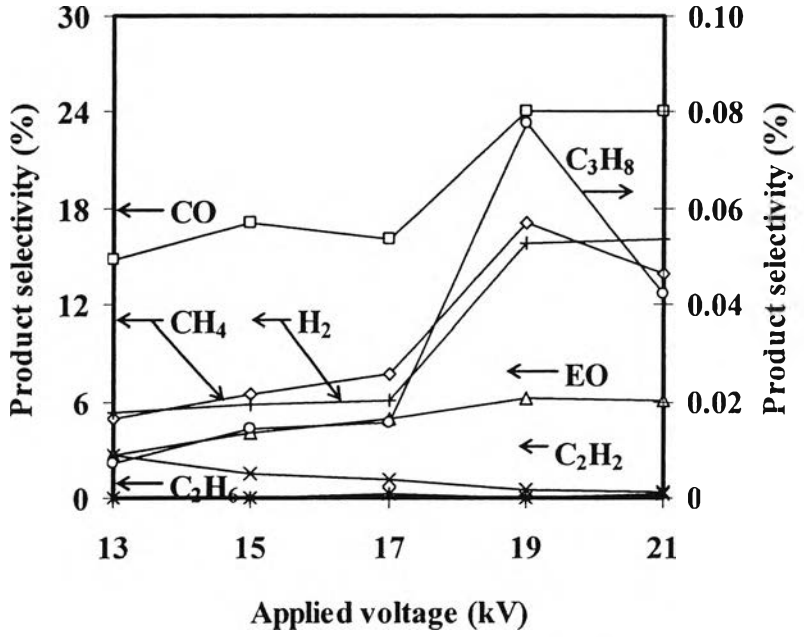

Figure 4.13 Product selectivities as a function of applied voltage (molar ratio of O_2/C_2H_4 = 1/1; feed flow rate = 50 cm^3/min; electrode gap distance = 10 mm; and input frequency = 500 Hz).

4.1.4.2 Comparison of Specific Power Consumption for Different Applied Voltages

Figure 4.14 shows the effect of applied voltage on the power consumptions. With increasing applied voltage, the power consumption per molecule of converted C_2H_4 remained almost unchanged, whereas the power consumption per molecule of produced C_2H_4O substantially decreased. As shown above about the slight increase in ethylene conversion, this might insignificantly affect the power consumption to convert ethylene molecule. In contrast, an increase in the selectivity for C_2H_4O was comparatively high as increasing the applied voltage, resulting in lower power consumption per molecule of produced C_2H_4O.

From the results, the applied voltage of 19 kV was selected to be the optimum value because this voltage provided reasonably high conversions of C_2H_4 and O_2, and the highest selectivity and yield for ethylene oxide. At a higher voltage, it did not affect any of reactant conversion, ethylene oxide selectivity, and

ethylene oxide yield. Moreover, at the applied voltage of 19 kV, the lowest power consumption per C_2H_4O molecule produced was obtained.

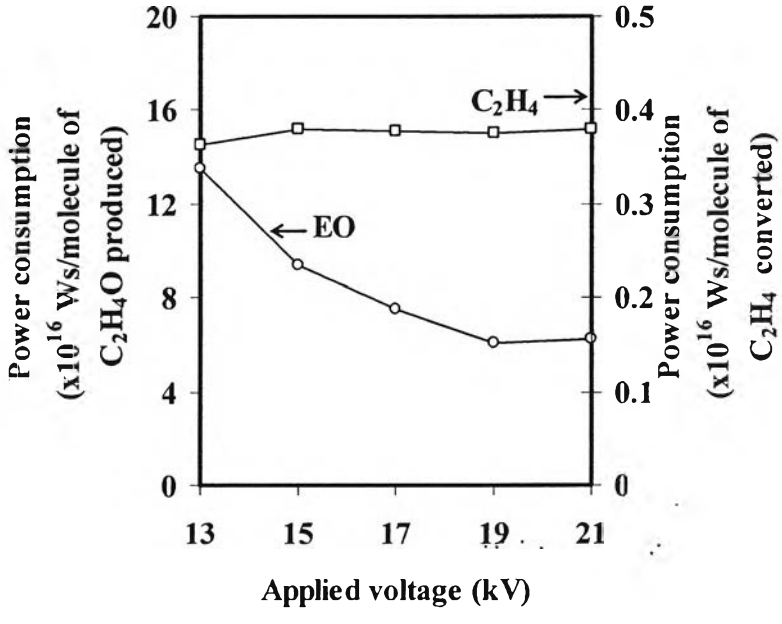

Figure 4.14 Comparison of specific power consumptions for different applied voltages (molar ratio of O_2/C_2H_4 = 1/1; feed flow rate = 50 cm^3/min; electrode gap distance = 10 mm; and input frequency = 500 Hz).

4.1.5 Effect of Electrode Gap Distance

The effect of electrode gap distance was studied under the optimum conditions achieved above; an O_2/C_2H_4 molar ratio of 1/1, a feed flow rate of 50 cm^3/min, an input frequency of 500 Hz, and an applied voltage of 19 kV. The lowest electrode gap distance for the studied DBD system was limited at 10 mm due to its configuration. At an electrode gap distance higher than 14 mm, the generated plasma became unfavorably non-uniform. Therefore, the reaction experiments were conducted in the range of electrode gap distance between 10 and 14 mm in order to determine the effect of the electrode gap distance.

4.1.5.1 Effect of Electrode Gap Distance on Ethylene and Oxygen Conversions, Ethylene Oxide Yield, and Product Selectivities

The effect of electrode gap distance on the C_2H_4 and O_2 conversions and C_2H_4O yield is illustrated in Figure 4.15. The ethylene conversion and ethylene oxide yield tended to decrease with increasing the electrode gap distance, whereas the oxygen conversion remained almost unchanged. The explanation for slight ethylene conversion decrement is that a wider electrode gap distance results in a higher residence time for several hydrocarbon species to recombine via coupling reactions, including backward reaction to form ethylene, causing lower conversion of ethylene. The unexpected nearly constant O_2 conversion with increasing electrode gap distance can be explained in that as shown in Figure 4.16, because the current slightly increased with increasing the electrode gap distance, it was sufficient for breaking the oxygen molecules despite flowing in a wider electrode gap distance with high probability of backward reaction, resulting in insignificantly affecting the oxygen conversion when varying the electrode gap distance in the investigated range. This means that for the O_2 conversion, the higher probability in converting O_2 molecules due to higher electron density might balance with the higher probability in oxygen active species recombination due to a longer residence time of gas flow. The expected increase in current, i.e. electron density, might be contributed to the special characteristic of the DBD system containing the dielectric plate, as well as the various compositions of gaseous species inside the plasma zone. At a higher electrode gap distance, the dielectric plate might sustain the discharge a little bit more effectively due to less loss of electrons via various reactions, under the identical input frequency and applied voltage.

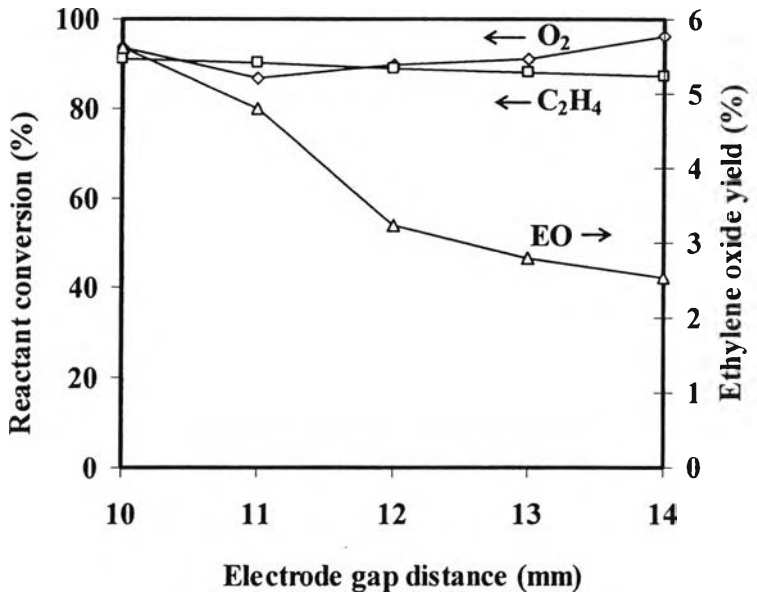

Figure 4.15 Conversions of ethylene and oxygen and yield of ethylene oxide as a function of electrode gap distance (molar ratio of O_2/C_2H_4 = 1/1; feed flow rate = 50 cm^3/min; applied voltage = 19 kV; and input frequency = 500 Hz).

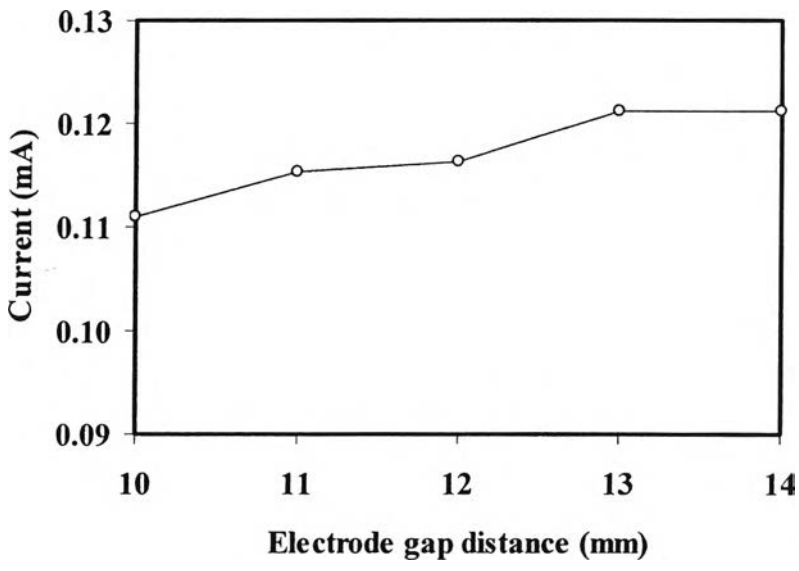

Figure 4.16 Effect of electrode gap distance on generated current (molar ratio of O_2/C_2H_4 = 1/1; feed flow rate = 50 cm^3/min; applied voltage = 19 kV, and input frequency = 500 Hz).

The effect of electrode gap distance on the selectivities for C_2H_4O, CO, H_2, CH_4, C_2H_2, C_2H_6, and C_3H_8 is shown in Figure 4.17. The selectivities for C_2H_4O, CO, H_2, and CH_4 decreased with increasing gap distance while the opposite trend was observed for C_2H_2, C_2H_6, and C_3H_8. These might be imply that when increasing electrode gap distance, the opportunity of coupling reactions might more favorably occur as secondary reactions than partial oxidation, as above explained.

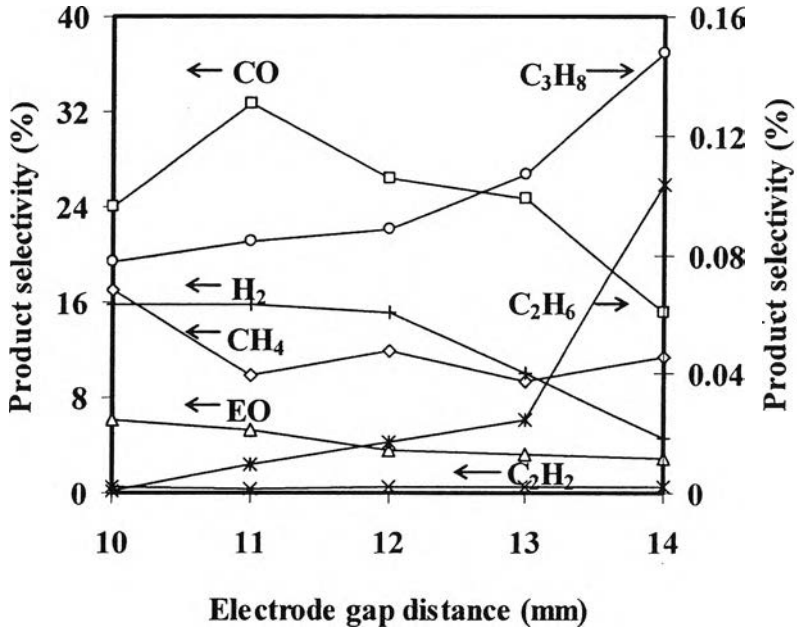

Figure 4.17 Product selectivities as a function of electrode gap distance (molar ratio of O_2/C_2H_4 = 1/1; feed flow rate = 50 cm^3/min; applied voltage = 19 kV; and input frequency = 500 Hz).

4.1.5.2 Comparison of Specific Power Consumption for Different Electrode Gap Distances

Figure 4.18 shows the effect of electrode gap distance on the power consumptions. It is clearly seen that both the power consumptions per molecule of converted C_2H_4 conversion and per molecule of produced C_2H_4O substantially increased with increasing electrode gap distance. A higher electrode gap distance caused a higher probability of secondary reactions, which unavoidably used up some power. From the results, the electrode gap distance of 10 mm was

considered as an optimum value because at 10 mm gap distance, the highest C_2H_4O selectivity and C_2H_4O yield with the lowest power consumption per C_2H_4O molecule produced were achieved.

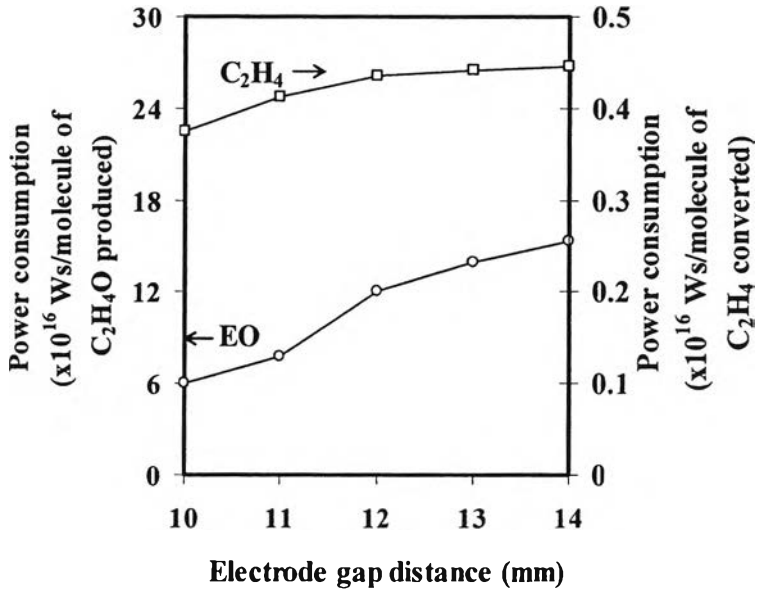

Figure 4.18 Comparison of specific power consumptions for different electrode gap distances (molar ratio of O_2/C_2H_4 = 1/1; feed flow rate = 50 cm^3/min; applied voltage = 19 kV; and input frequency = 500 Hz).

4.2 Comparison of Reaction Activity Performance under Dielectric Barrier Discharge and Corona Discharge

For both types of plasma reactor with fixed discharge gap between two electrodes, gas phase reactions induced by the discharge mainly contribute to the reactant conversions. In a plasma discharge system, most of discharge energy is used to produce and accelerate electrons, which then react with gas molecules to generate highly active species (metastables, radicals, and ions). Ethylene and oxygen are therefore chemically activated directly by electron collisions. In this work, a comparison of ethylene epoxidation using two types of plasma reactor, namely dielectric barrier discharge and corona discharge, was studied in order to investigate a suitable reactor system providing the highest ethylene oxide yield. For the

dielectric barrier discharge reactor, only sole plasma system was examined, whereas both sole plasma and combined catalytic-plasma systems were comparatively used for the corona discharge reactor. From the previous work reporting the ethylene epoxidation activity using a combined catalyst and corona discharge system (Tansuwan, 2007), it was found that this plasma system operated with the presence of 12.5 wt.% Ag/(LSA)α-Al_2O_3 catalyst provided the highest selectivity for ethylene oxide. In this work, various bimetallic catalysts prepared based on the Ag catalyst using many promoters, which were reported in several literatures to be catalytically active for the ethylene epoxidation, were investigated for the corona discharge system as to compare with the dielectric barrier discharge sole plasma system. All investigated catalysts for the corona discharge system were Ag/(LSA)α-Al_2O_3, Cs-Ag/(LSA)α-Al_2O_3, Cu-Ag/(LSA)α-Al_2O_3, and Au-Ag/(LSA)α-Al_2O_3. All experiments were carried out at ambient temperature and atmospheric pressure under the above obtained optimum conditions; an O_2/C_2H_4 molar ratio of 1/1, a feed flow rate of 50 cm^3/min, an input frequency of 500 Hz, an applied voltage of 19 kV, and an electrode gap distance of 10 mm.

4.2.1 Effect of Type of Plasma Reactor in the Absence and Presence of Catalysts on Ethylene and Oxygen Conversions, Ethylene Oxide Yield, and Product Selectivities

Figure 4.19 shows the reactant conversions and the ethylene oxide yield between the two different types of reactor. It was found that under the corona discharge, the conversions of ethylene and oxygen and the yield of ethylene oxide were significantly enhanced by using all bimetallic catalysts as compared with the monometallic Ag catalyst. However, under the dielectric barrier discharge, both the reactant conversions were observed to be significantly higher than those under the corona discharge, even though the latter was operated with many types of reported catalytically active catalysts. Moreover, it was interestingly found that the yield of ethylene oxide under the dielectric barrier discharge was more preferably obtained.

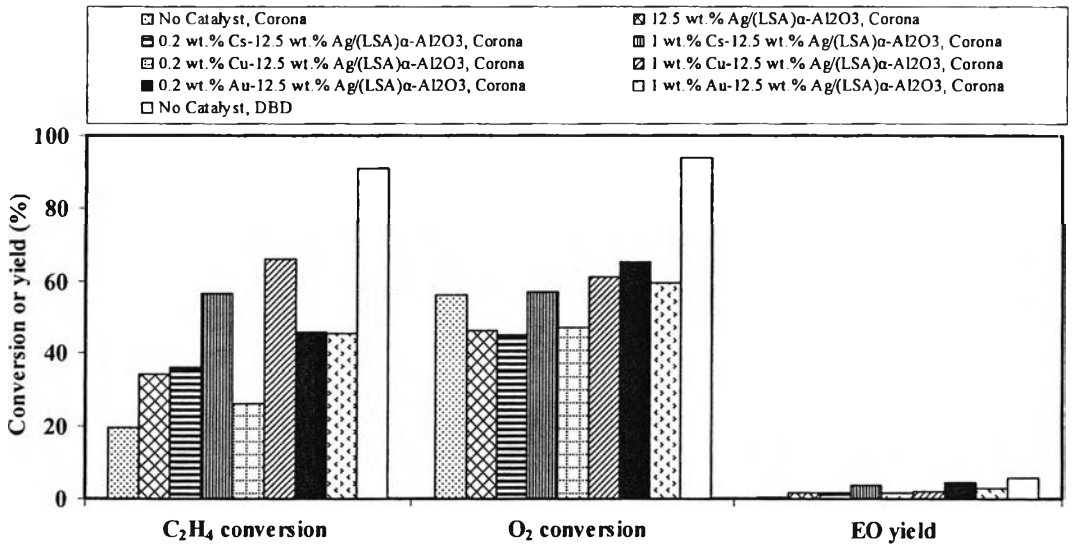

Figure 4.19 Comparison of reactant conversions and ethylene oxide yield between dielectric barrier discharge and corona discharge systems (molar ratio of O_2/C_2H_4 = 1/1; feed flow rate = 50 cm^3/min; applied voltage = 19 kV; input frequency = 500 Hz; and electrode gap distance = 10 mm).

Figure 4.20 comparatively shows the product selectivities. It can be seen that under the corona discharge, type of catalysts significantly affected the selectivities for main investigated products, i.e. C_2H_4O and CO. The bimetallic 0.2 wt.% Au-12.5 wt.% Ag/(LSA)α-Al_2O_3 combined with plasma was shown to favor the partial oxidation reaction to form ethylene oxide as compared with other catalysts. Moreover, it still provided a relatively low amount of CO. When comparing with the dielectric barrier discharge, although the slightly lower C_2H_4O selectivity was obtained, the C_2H_4O yield was considerably higher due to the higher C_2H_4 conversion. In addition, the CO selectivity was lower for the operation under the dielectric barrier discharge. Interestingly, H_2 was also more significantly formed under this type of plasma reactor. Therefore, it can be concluded that the sole plasma of dielectric barrier discharge system exhibited the superior performance for the ethylene epoxidation due to higher ethylene conversion, higher ethylene oxide yield, and lower amount of CO produced. This might be explained in that the plasma distribution in form of microdischarge for the dielectric barrier discharge system is much more uniform over the entire surface of the two parallel electrodes than the

corona discharge system, which was an advantage of the dielectric barrier discharge over the corona discharge.

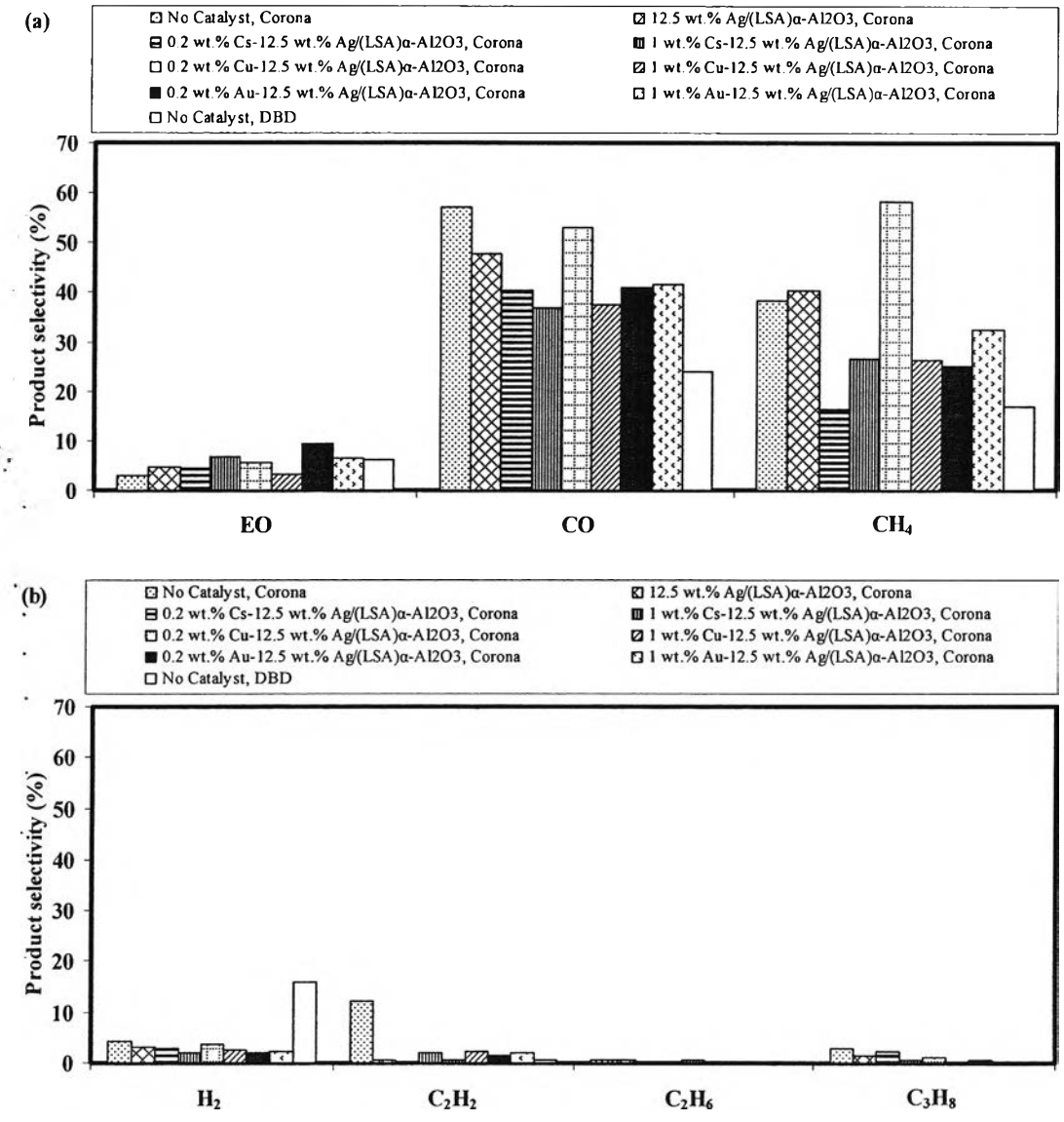

Figure 4.20 Comparison of product selectivities for (a) C_2H_4O, CO, and CH_4 and (b) H_2, C_2H_2, C_2H_6, and C_3H_8 between dielectric barrier discharge and corona discharge systems (molar ratio of O_2/C_2H_4 = 1/1; feed flow rate = 50 cm^3/min; applied voltage = 19 kV; input frequency = 500 Hz; and electrode gap distance = 10 mm).

4.2.2 Comparison of Specific Power Consumption for Different Types of Plasma Reactor in the Absence and Presence of Catalysts

Figure 4.21 illustrates the power consumptions per C_2H_4O molecule produced and per C_2H_4 molecule converted. In general observation, it was found that the power consumptions were varied upon the types of plasma reactor. The power consumption per C_2H_4O molecule produced was almost two orders of magnitude higher than that per C_2H_4 molecule converted and therefore should be mainly used for comparison of the process performance. For the corona discharge system, the presence of catalysts significantly helped reduce the power consumptions, as can be especially seen from the lowest power consumption per C_2H_4O produced when operating the corona discharge with the 0.2 wt.% Au-12.5 wt.% Ag/(LSA)α-Al_2O_3 catalyst, which exhibited good epoxidation performance shown above. The power consumption per C_2H_4 molecule converted was also acceptably low. Interestingly, both the power consumptions for the sole plasma system of the dielectric barrier discharge were obviously lower than those for the combined catalytic-plasma system of corona discharge, i.e. the lowest among all investigated systems. In conclusion, the dielectric barrier discharge reactor was therefore more suitable for ethylene oxide production than the corona discharge reactor, even though it was not operated with any catalytically active catalysts. It provided the highest conversions of C_2H_4 and O_2, the highest yield of ethylene oxide, the lowest amount of CO produced, and also the lowest power consumptions both per C_2H_4O molecule produced and per C_2H_4 molecule converted.

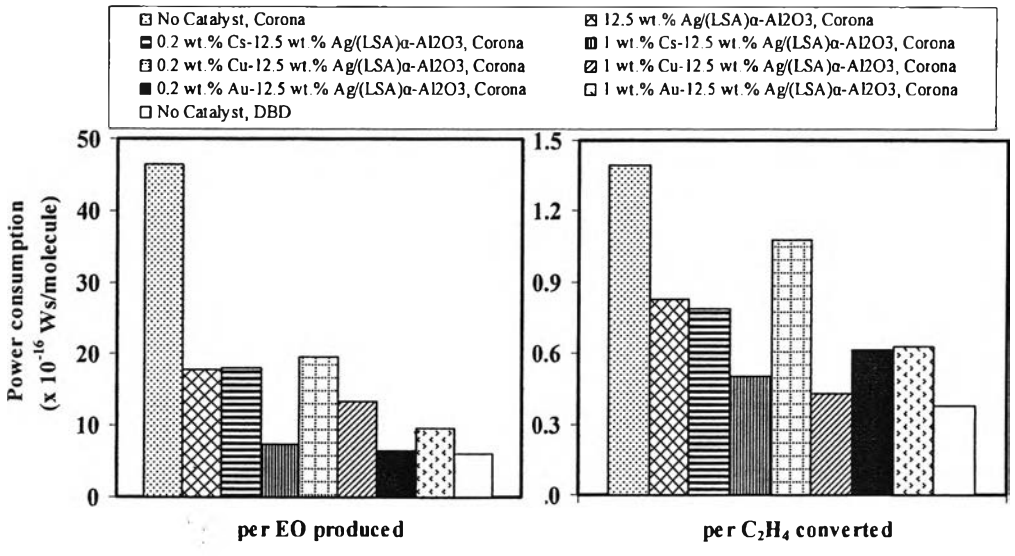

Figure 4.21 Comparison of power consumptions per ethylene oxide molecule produced and per ethylene molecule converted between dielectric barrier discharge and corona discharge systems (molar ratio of O_2/C_2H_4 = 1/1; feed flow rate = 50 cm^3/min; applied voltage = 19 kV; input frequency = 500 Hz; and electrode gap distance = 10 mm).

4.2.3 Characterizations of Catalysts Used in Corona Discharge System

In this study, four types of catalysts, namely Ag/(LSA)α-Al_2O_3, Cs-Ag/(LSA)α-Al_2O_3, Cu-Ag/(LSA)α-Al_2O_3, and Au-Ag/(LSA)α-Al_2O_3, were used for investigating the ethylene epoxidation activity in the combined catalytic and corona discharge system.

The BET surface areas of all investigated Ag/(LSA)α-Al_2O_3-based catalysts are shown in Table 4.1. The results indicate that when the three second metals were sequentially loaded on the Ag/(LSA)α-Al_2O_3 catalyst, the surface areas of all bimetallic catalysts slightly increased. This implies that the loaded metals might well disperse on the Ag/(LSA)α-Al_2O_3 catalyst. The surface areas of these well-dispersed metals might attribute to the slight increase in the surface area of the initially prepared catalyst with extremely low surface area. The insignificantly different surface areas of all catalysts might play less important role than the property of the metals themselves on the epoxidation activity.

The amount of coke formed on the spent catalysts is also included in Table 4.1. It can be clearly seen that there was, in overall, extremely low amount of coke formed for all catalysts, propably due to the low catalyst surface area available for coke deposit. However, the Au-Ag/(LSA)α-Al_2O_3 catalysts, which exhibited the comparatively good epoxidation performance, tended to induce more coke formation.

Table 4.1 BET surface area and amount of coke formed for all investigated catalysts

Catalyst	BET surface area (m^2/g)	Coke formation[a] (%)
12.5 wt.% Ag/(LSA)α-Al_2O_3	0.28	0.26
0.2 wt.% Cs-12.5 wt.% Ag/(LSA)α-Al_2O_3	0.33	0.11
1 wt.% Cs-12.5 wt.% Ag/(LSA)α-Al_2O_3	0.44	0.16
0.2 wt.% Cu-12.5 wt.% Ag/(LSA)α-Al_2O_3	0.39	0.14
1 wt.% Cu-12.5 wt.% Ag/(LSA)α-Al_2O_3	0.74	0.22
0.2 wt.% Au-12.5 wt.% Ag/(LSA)α-Al_2O_3	0.33	0.75
1 wt.% Au-12.5 wt.% Ag/(LSA)α-Al_2O_3	0.42	1.07

[a] molar ratio of O_2/C_2H_4 = 1/1; feed flow rate = 50 cm^3/min; applied voltage = 19 kV; input frequency = 500 Hz; and electrode gap distance = 10 mm

In this study, TEM was employed to mainly observe the morphology and mean particle size of Ag on the surface of studied catalysts. The results from the TEM analysis showed that Ag particles are highly dispersed on the alumina support for all catalysts. As exemplified in Figure 4.22, TEM micrographs of 0.2 wt.% Au-12.5 wt.% Ag/(LSA)α-Al_2O_3 catalyst, which exhibited the superior activity toward the ethylene epoxidation as explained above, revealed mean Ag particle size of approximately 6 nm for fresh catalyst and approximately 8 nm for spent catalyst. These suggest that the silver agglomeration occurred after the activity test due to its

relatively larger particle size on the spent catalyst. This Ag agglomeration on the surface of spent catalyst is believed to result from the high energy intensity of the corona discharge used in this study. For non-thermal AC plasma, the bulk gas temperature is comparatively low; however, the energetic electrons may have energy ranging from 1 to 10 eV, which corresponds to extremely high temperatures of about 10,000 and 100,000 K (Rosacha et al., 1993). Therefore, the catalyst surface has high probability to be collided intermittently with these high-temperature electrons, causing the increase in temperature on scattering micro-sized spots in a very short period throughout the catalyst surface and subsequently resulting in the Ag agglomeration.

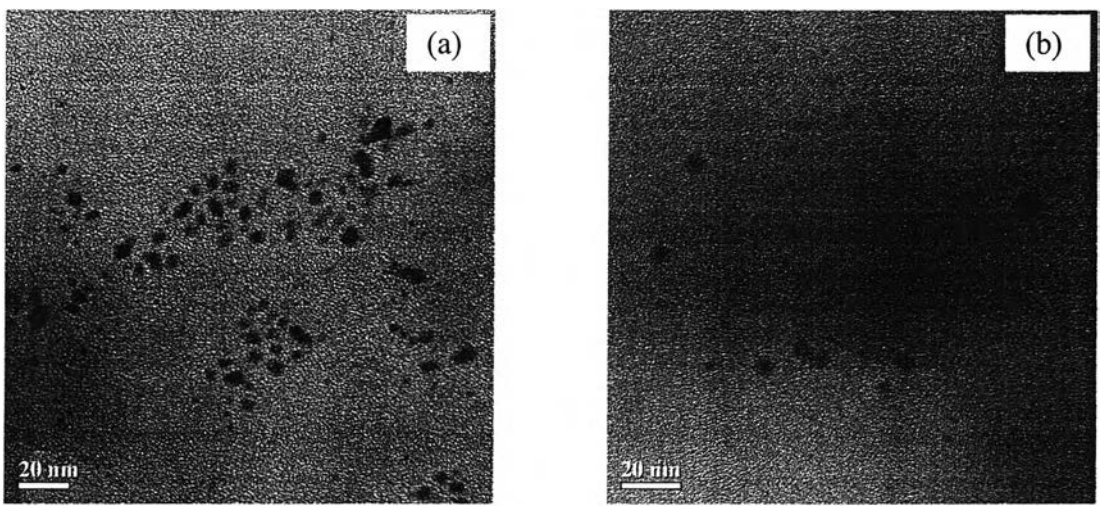

Figure 4.22 TEM images of Ag particles on (a) fresh and (b) spent 0.2 wt.% Au-12.5 wt.% Ag/(LSA)α-Al_2O_3 catalyst.

The XRD patterns of all studied catalysts are shown in Figure 4.23. All bimetallic catalysts showed the same XRD patterns as the monometallic Ag/(LSA)α-Al_2O_3 catalyst, mainly consisting of α-Al_2O_3 and Ag phases. For the Au-Ag/(LSA)α-Al_2O_3, the peaks corresponding to Au phase were obviously observed. However, for both Cs-Ag/(LSA)α-Al_2O_3 and Cu-Ag/(LSA)α-Al_2O_3 catalysts, there was no clear evidence of any peaks corresponding to Cs and Cu. This is plausibly due to their light mass as compared with Au at the same wt.% loadings.

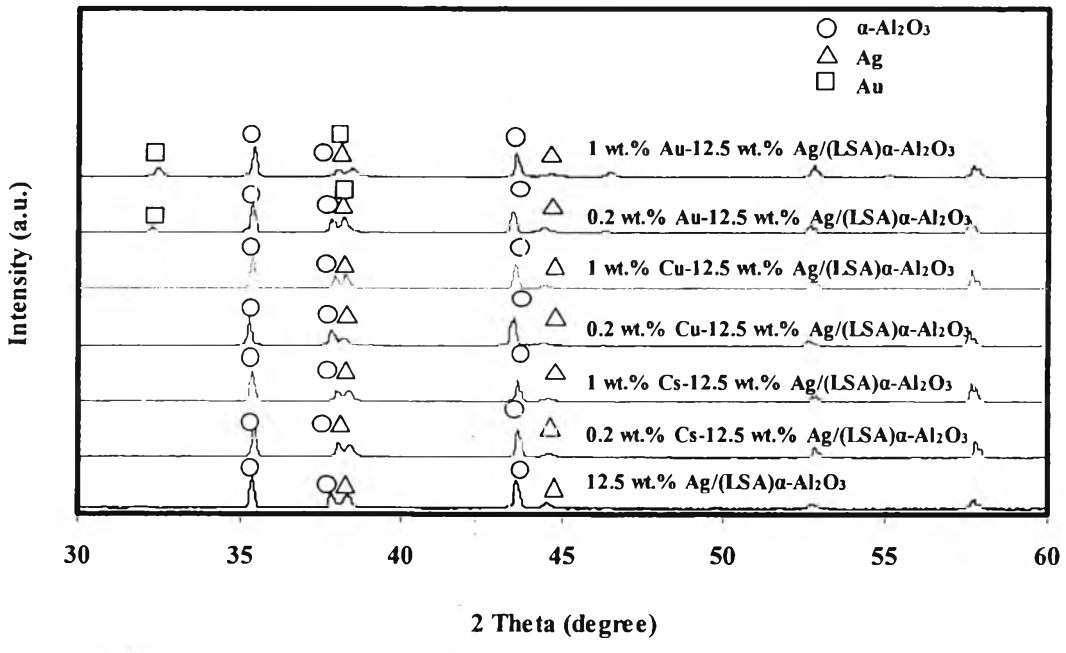

Figure 4.23 XRD patterns of all studied catalysts.